Mountain-Originated Mesoscale Precipitation System in Northern Taiwan: A Case Study 21 June 1991

BEN JONG-DAO JOU[1]

ABSTRACT

In the late morning of 21 June 1991, a convective precipitation system developed in the mountainous area in northern Taiwan. The convective precipitation system was organized into a northeast-southwest oriented mesoscale line feature along the western mountain slope at a later time. More than 120 mm of rainfall poured down on Taipei and Keelong cities within 3 hours. The initiation, development, organization and dissipation of the storm were detected by a C-band Doppler weather radar on the northwest coast of Taiwan. In this paper, the role of mountains in organization and propagation of the mesoscale precipitation system is studied by using the Doppler radar data.

The storm initiated at the mountain peak area, propagated down the terrain slope and brought heavy rain to the basin and plain areas. In the early stage, advection dominated. The precipitation system developed along the mean low-to-middle tropospheric winds into a northeast-southwest convective line. When precipitation-induced outflows occurred, the interaction between the upslope winds and the storm-generated outflows dominated storm propagation. At this stage, the precipitation system moved northwestward downslope. Reaching the foothills of the mountains, the storm was intensified dramatically by sea-breeze circulation. In the basin area, the interaction between the storm-generated outflows and the environmental low-level flows dominated the storm development. At this stage, the storm was quasi-stationary. Deep cumulonimbus clouds continually reformed over the southwest quadrant, moved northeastward and produced copious rainfall in the same region.

The vertical structure of the convective precipitation system was also examined in this study. The strong reflectivity region in the storm was first found at an altitude of about 2 km and extended well above 12 km. The convective updrafts, inferring from the uplift of the westerly momentum in the middle troposphere associated with the penetrated sea-breeze circulation, tilted slightly downshear at the leading edge of the storm. The existence of convective downdrafts located just behind the updraft region was also indicated by the Doppler radar observations of pronounced precipitation-induced divergence outflows near the surface and also confirmed by surface observations at Taipei station. The stratiform rain area was at the rear portion of the precipitation system and was not well-organized. No bright band signature was found in the reflectivity data.

(Key words: Heavy precipitation, Mountain convection, Northern Tawian, Doppler radar, Thermally-induced upslope winds and sea-breeze)

---

[1] Department of Atmospheric Sciences, National Taiwan University, Taipei, Taiwan, R.O.C.

1. INTRODUCTION

In 1991, a pilot program of the Post-TAMEX Forecast Experiment was held during May and June. The Post-TAMEX Forecast Experiment was a continuation of the Taiwan Area Mesoscale EXperiment (TAMEX) field program held in 1987 (Kuo and Chen, 1990). One of the objectives of this pilot program was to exercise the forecast skills derived from the scientific results of TAMEX on the torrential rain-producing mesoscale precipitation systems (MPSs) associated with the Mei-Yu front or generated by local circulations and rugged terrains (see special issue of TAMEX in Monthly Weather Review, November 1991).

The first one and half months of the exercise was a rather quiet Mei-Yu season. No significant events associated with the Mei-Yu front were encountered. Scattered showers triggered by local circulations or sloping terrains were the dominant precipitation features in the period. In fact, the local weather authority declared the year was an empty-Mei-Yu year and there was a severe drought in southern Taiwan. At the end of June, the situation changed abruptly and became quite interesting. In the late morning of 21 June 1991, a convective precipitation system developed in the mountainous area in northern Taiwan. The convective precipitation system organized into a northeast-southwest (NE-SW) mesoscale line feature along the western mountain slope in northern Taiwan. More than 120 mm (about 4.7 inches) rain poured down on Taipei and Keelong (a harbor on the northern tip of Taiwan) within 3 hours. The maximum rainfall intensity on the record was 40 mm (1.6 inches) within 10 minutes (Keelong station). Torrential rain fell on the Taipei basin and Keelong city that afternoon. The case caught our attention not only because it caused a severe flash flood in the most populated metropolitan area in Taiwan, but it provided an opportunity to study the role of mountains in organization and propagation of the mesoscale precipitation systems in northern Taiwan since the initiation, development, organization, and dissipation of the storm were within the detection limit of a C-band Doppler weather radar located on the northwest coast of Taiwan.

Taiwan is located in the subtropical latitudes of the western North Pacific. In the late spring and summer, southwesterly monsoonal flows prevail. As suggested by Sun *et al.* (1991) and many others, these flows can interact with the Central Mountain Range (CMR) of Taiwan to produce significant mesoscale circulations in Taiwan and its surrounding area. Mesoscale precipitation systems are triggered by and organized closely with these circulations. Johnson and Bresch (1991) pointed out that the precipitation pattern in Taiwan in Mei-Yu season (May and June) has a pronounced diurnal variability component. Most rainfall over the mountains occurs during the afternoon and evening hours and rainfall on the coastal plains is shifted to slightly earlier times. They attributed this diurnal variation of precipitation to the land-sea breeze circulation interaction with the prevailing flows. In addition, Johnson and Bresch examined the evolution of the sea breeze and the development of the afternoon mixed layer on a synoptically undisturbed day when afternoon thunderstorms occurred over the island. The presence of daytime sea breeze is important in moistening the planetary boundary layer which is favorable for the initiation of thunderstorms in the afternoon.

By using a two-dimensional Durran and Klemp (Durran and Klemp, 1982) type cloud model, Chen *et al.* (1991) studied the orographic effect on mesoscale precipitation systems in northern Taiwan in Mei-Yu season. In the case studied, the new convective cells formed over the sloping area to the west of the mountain crest and propagated east toward the mountain top. The new cells then merged with the old cells over the mountain and moved eastward and dissipated. The heavy rain was brought to the sloping and mountainous areas. The sensitivity

study pointed out that abundance of low and mid-level moisture supply, moderate low-level winds, correct size of mountain, and strong surface heating induced upslope winds are all important factors in sustaining a long-lived mesoscale precipitation system over northern Taiwan. The convective system studied by Chen *et al.* behaved quite differently from the present case. In this study, instead of dropping heavy rain over sloping and mountainous areas, the convective storms first formed in the mountainous area, propagated westward downslope, and then brought heavy rain to the basin and foothill areas. An understanding of the causes of the differences in storm initiation, movement and propagation in the case of Chen *et al.* and the present one is one of the objectives of this study.

According to Cotton and Anthes (1989), storm movement and propagation can be classified into three different mechanisms: (i) translation or advection, (ii) forced propagation, and (iii) autopropagation. Translation or advection is the process whereby a storm is blown along by the mean wind as it evolves through its lifetime. Forced propagation refers to the sustained regeneration of a convective storm by some external forcing mechanism usually larger in scale than the convective storm. Examples include fronts, rainband convergence in midlatitude cyclones, sea-breeze fronts, and convergence associated with mountains. Often the systems providing the forced propagation have lifetimes much longer than individual thunderstorms. Autopropagation refers to the process in which a thunderstorm can regenerate itself or cause the generation of similar storm cells within the same general system. Examples include downdraft forcing and gust fronts, and development of vertical pressure gradients due to storm rotation. Most convective systems are affected by all three mechanisms of movement and propagation for at least some part of their lifetime. In this study, a mountain-originated mesoscale convective precipitation system in northern Taiwan is presented. The movement and propagation of the precipitation system is delineated by using single-Doppler radar located at CKS International Airport in northern Taiwan. The possible mechanisms related to the interactions among the environmental winds, the sea-breeze circulation, the mountain slope, and the storm-generated outflows are discussed. In addition, the structure and evolution of convection associated with the mesoscale precipitation system is also examined.

2. DATA

Data used in this study were obtained from a C-band Doppler weather radar at CKS International Airport of the Civil Aeronautic Administration of Taiwan (CAA Doppler radar). The location of the radar is shown in Figure 1. Plan-position indicator (PPI) reflectivity and radial wind data, in a time interval of 30 minutes, were gathered. Hourly satellite IR imageries, soundings of Panchiao station (46692), and surface weather and precipitation data from stations over northern Taiwan were also used.

3. CASE DESCRIPTION

3.1 Precipitation Pattern

Figure 1 shows the six-hour accumulated rainfall (end time is 1800 LST) distribution over northern Taiwan during the period of interest. It shows there were two major precipitation centers, one in the Keelong area and the other in the Taipei basin. The rain at Keelong (46694) started at 1300 LST, 21 June 1991 with a trace amount and peaked to 28.5 mm at
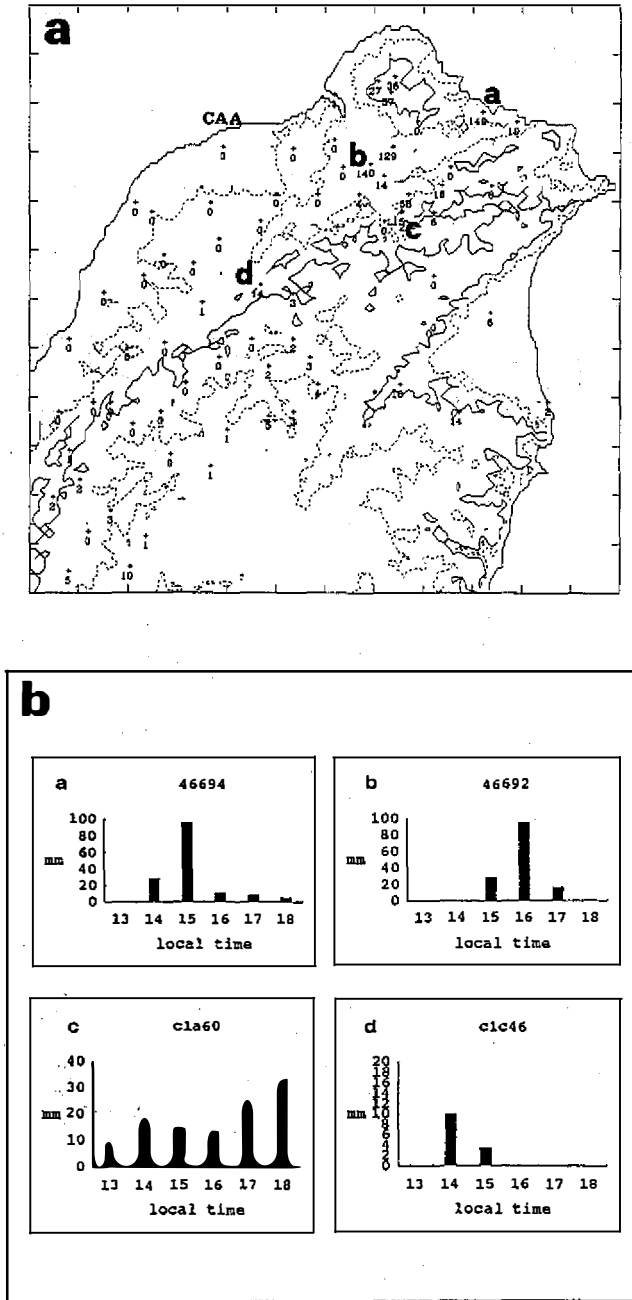
Fig. 1. (a) Six-hourly (end time is 1800 LST) accumulated rainfall (in mm) in northern Taiwan. The contours are topographic heights above sea level, 200 m, 500 m, and 1500 m, respectively. (b) Hourly rainfall distribution from selected stations in northern Taiwan. The geographic locations of each station are marked in (a).

end of the hour. In the next hour, the accumulated rainfall hit the record high with rainfall intensity of 95 mm h^{-1}. The total accumulated rain between 1300-1600 LST at Keelong was 134.4 mm. The rain at Taipei station (46692) started at 1400 LST, an hour later than in Keelong city. Within 3 hours (ending at 1700 LST), the total accumulated rainfall was 140 mm with maximum rainfall rate of 94.5 mm h^{-1}. The life of the precipitation system was relatively shorter than the frontal precipitation system usually occurring in this season but lasted much longer than an individual thunderstorm. The heavy rain associated with the precipitation system was rather concentrated in terms of spatial and temporal scales. This precipitation character makes a difficult flash flood nowcast problem for the local weather forecasters.

3.2 Synoptic Conditions

The surface weather map at 0000 UTC (0800 LST) 21 June 1991 (Figure 2a) showed the surface front located some distance north of Taiwan. The front approached the island slowly. Deep but weak southwest monsoonal flows (up to 400 hPa) with warm and moist air prevailed in northern Taiwan. The morning sounding of Panchiao (46692) (Figure 2b) showed very low lifting condensation level (LCL=988 hPa) with surface water vapor mixing ratio of 20 g kg^{-1}. The level of free convection was also very low (LFC=977 hPa). The convective available potential energy (CAPE), estimated by hypothetically lifting a surface air parcel through a pseudo-adiabatic process, showed a relatively large number, e.g., 1818 $m^2 s^{-2}$, indicating a strongly convective-unstable atmosphere. The hodograph (Figure 2c) indicated that the lower tropospheric winds were southwesterlies and rather weak, most of them were less than 5 m s^{-1} below 900 hPa. No pre-frontal low-level jet existed.
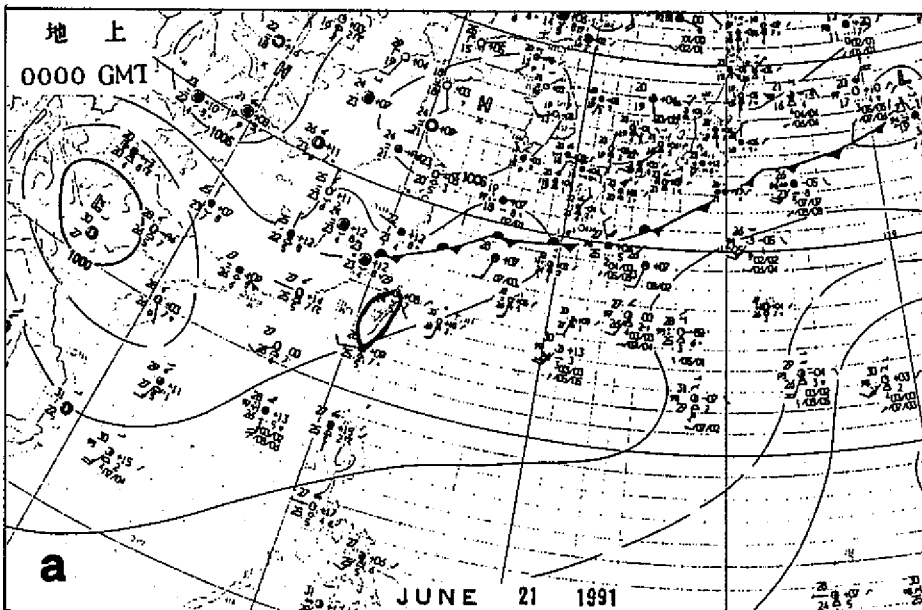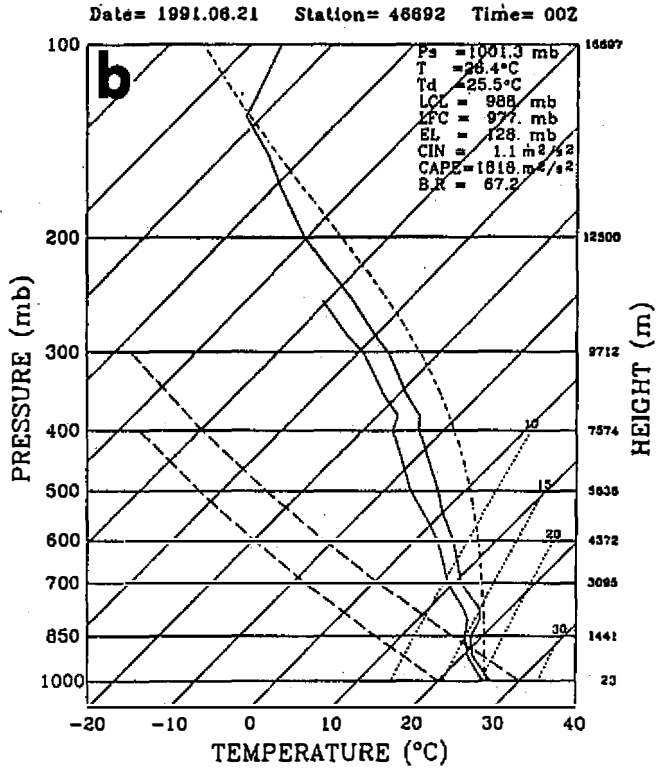

Fig. 2. (a) Surface weather map for 0000 UTC (0800 LST) 21 June 1991. (b) The skew T-log P presentation of sounding from Panchiao (46692) at 0800 LST 21 June. The short broken line represents the moist-adiabatic curve a hypothetically ascending surface parcel would have. (c) The hodograph of Panchiao sounding on 0800 LST 21 June.

Date= 1991.06.21   Station= 46692   Time= 00Z

Hodograph Map

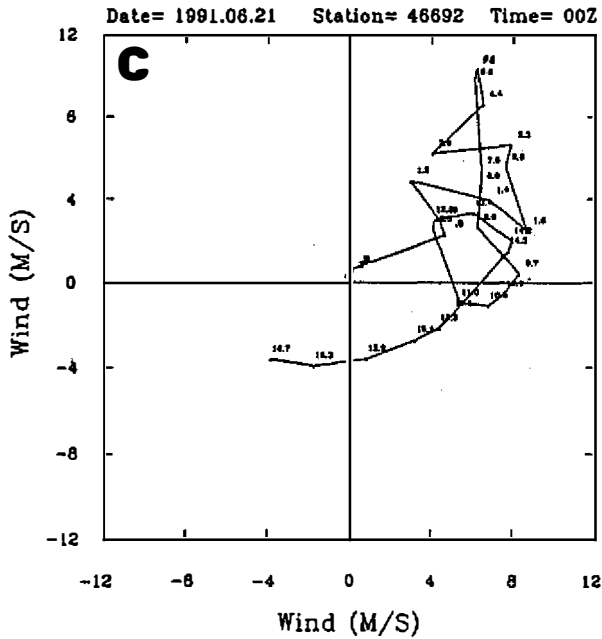Date= 1991.06.21   Station= 46692   Time= 00Z

Fig. 2. (Continued.)

3.3 Local Wind Analysis

Daytime hourly local wind analyses on 21 June in northern Taiwan are given in Figure 3. In these figures, the geographic map has been rotated 45° clockwise for convenience, hence, the right side of the map is northeast. At 11 am (Figure 3b), the surface winds were weak southwesterlies along the coastal region. At noon time (Figure 3c), the coastal winds turned clockwise with a stronger landward wind component indicating the existence of sea-breeze circulation. The sea-breeze circulation penetrated further inland and strengthened its intensity at 1 pm as shown by the turning of surface winds to more westerlies at the two stations in the Taipei basin (Figure 3d). Correspondingly, the surface temperature at Taipei station increased from 26°C at 8 am and reached 33°C near noontime. These observations suggested that, on the morning of 21 June, thermally-driven sea-breeze circulation prevailed. The increase of surface temperature before noontime is mostly due to solar heating in northern Taiwan.

Surface winds in the Taipei basin had experienced significant direction changes at 2 pm (Figure 3f, 180° out of phase). This direction change accompanied the starting of precipitation at these two stations. This observation suggested that the local wind structure in northern Taiwan could be modified significantly by the passage of the convective precipitation system in the Mei-Yu season.

3.4 Evolution of the Precipitating System

In Figure 4, a sequence of 3 km constant-altitude plan-position indicator (CAPPI) radar-reflectivity maps from CAA C-band Doppler radar are given to show time evolution of the mesoscale precipitation system in northern Taiwan. The first echo was observed 30 km southeast of Taipei basin over the mountainous area at around 1100 LST (Figure 4a). The early development of the echoes (Figures 4b and c) were oriented in a NE-SW direction parallel to the mountain range and near the peak area. The echoes gradually evolved into a linear feature at around 1235 LST (Figure 4d). At 1305 LST (Figure 4e), a multi-cellular convective line system with several strong precipitation centers embedded within the line were observed. The precipitation system intensified rapidly and showed an explosive development as it reached the foothills. The major heavy precipitation area (defined by the equivalent reflectivity factor $Ze > 40$ dBZ, corresponding to a rainfall rate approximately 15 mm h^{-1}) became an elongated compound feature at 1405 LST (Figure 4g). The mesoscale precipitation system reached its mature stage (defined by the period when the precipitation area with $Ze > 45$ dBZ reached its maximum value) in the Taipei basin at around 1505 LST (Figure 4i). The precipitation system possessed strong reflectivity intensity during the period of 1505-1605 LST (Figures 4j and k) and dissipated afterwards.

There are several interesting phenomena associated with the evolution of the precipitation system. Firstly, the precipitation system at its mature stage delivered heavy rain over an area very similar to the geographic configuration of Taipei basin (Figure 4i). It occupied an area about 40 km long and 20 km wide. If estimated by the rainfall intensity of 15 mm h^{-1} during its mature stage, the total water deposited each hour into this area is twelve million metric tons! It is no surprise that even the Presidential Palace at the center of Taipei was flooded that afternoon.

Secondly, the precipitation system developed into a complex mesoscale structure after it reached the mature stage. The convective precipitation area extended northeastward along the mean low-to-middle tropospheric wind direction (see Figure 2c) and dissipated rapidly after
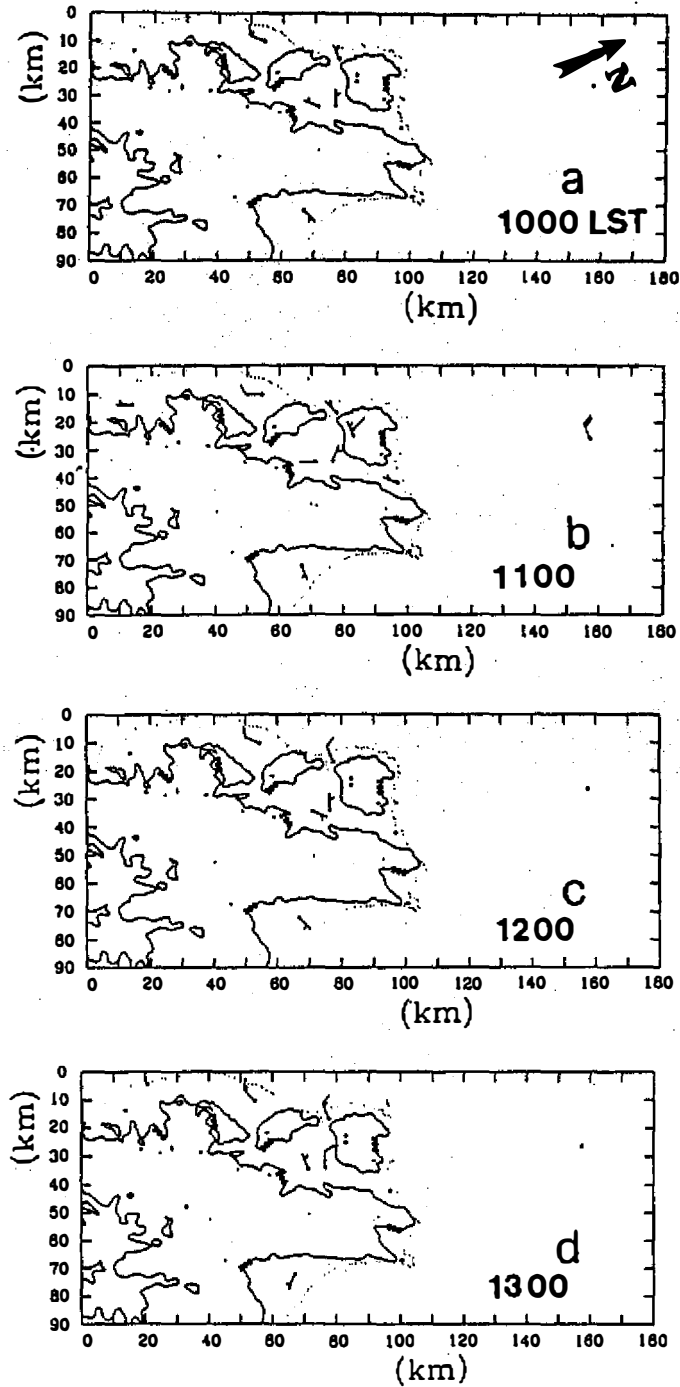
Fig. 3. Hourly local wind analysis in northern Taiwan from (a) 1000 LST to (h) 1700 LST, 21 June 1991. Full arrow is 5 m s^{-1} and half arrow is 2.5 m s^{-1}. The terrain contours are 200 and 1500 meters, respectively.
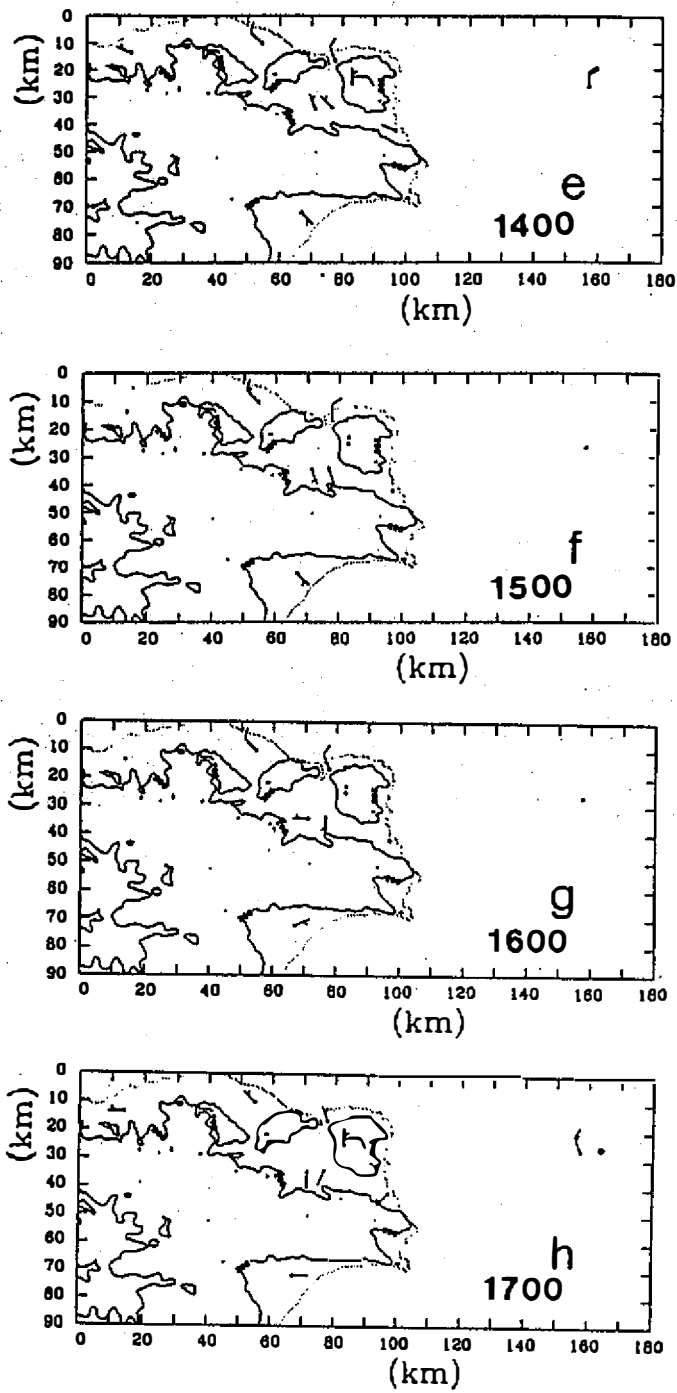
Fig. 3. (Continued.)

it moved into the ocean. In summary, the mesoscale precipitation system moved westward from the mountainous area toward the basin. Nevertheless, the precipitation system never reached the coastal area. These observed features seem to suggest the complicated relationship between the convective precipitation systems and the complex terrain of northern Taiwan.

Thirdly, the spatial scale of the precipitation echoes, at its early developing stage, was rather narrow, i.e., less than 10 km wide in the direction perpendicular to the storm system. After the storm reached its mature stage in the Taipei basin (Figures 4i and j), the precipitation echoes extended to its maximum horizontal scale (50 km wide). At this time, the major convective precipitation echoes were concentrated in the basin area and the weaker echoes associated with the stratiform precipitation were present to the east in the mountainous area. The stratiform precipitation areas associated with the system occurred in a large area only after the system started to decay (Figures 4n and 4o). It was also noted that although the environmental conditions were quite similar, the stratiform precipitation in this case had a much weaker intensity and shorter duration than what is usually observed in a tropical squall-line system (Gamache and Houze, 1982). Finally, in Figure 4l, the observations showed that there was secondary development of convection in the mountainous areas in late afternoon, which contributed significantly to prolonging the life of this mesoscale precipitation system.

Time evolution of clouds associated with the mesoscale precipitation system was given by the corresponding hourly enhanced IR satellite imageries shown in Figure 5. No discernible signatures of convective activities were observed in northern Taiwan until 1400 LST (0600 UTC). Two small deep-penetrated cumulonimbi were observed in northern Taiwan at 1400 LST. Rapid development of the individual convective system quickly merged together and formed a linear shape multi-cellular convective precipitation system with pronounced round-shape mesoscale anvil cloud (0800 UTC). The cold cloud top extended northeastward parallel to the flow at 200 hPa level. The clouds associated with the precipitation system dissipated rapidly after moving into the ocean.

4. STORM MOVEMENT AND PROPAGATION

From the description in last section, it is seen that the mesoscale precipitation system in northern Taiwan as a whole moved westward. However, a detailed examination of the reflectivity data shows that individual major precipitation centers, as defined by the entities in which radar reflectivity factors > 40 dBZ, moved differently. Figure 6 shows the 3 km reflectivity map at 1335 LST 21 June superimposed on terrain contours in northern Taiwan. Three major precipitation centers (called storms afterwards) over mountainous areas were identified. At this time, these storms were aligned and propagated westward down the mountain slope. We traced each individual storm's trajectory by using sequential CAPPI reflectivity maps with 30-minute intervals. The result is shown in Figure 7. It can be seen that each individual storm presented a quite different trajectory. To the south of Taipei, storm C moved northeastward to the lower land. To the east of Taipei, storms A and B both moved westward to the basin. Storm C had a propagation speed of 6.3 m s^{-1}, storm B (toward the Keelong city) had a speed of 3.4 m s^{-1}, while storm A had a speed of 2.3 m s^{-1} in the sloping area and moved very slowly in the Taipei basin. It is noted that storm A moved northwestward in the sloping area and moved southwestward in the Taipei basin. This direction change occurred over the foothills southeast of the Taipei basin, indicating a subtle relationship between storm propagation and the terrain surrounding the city.
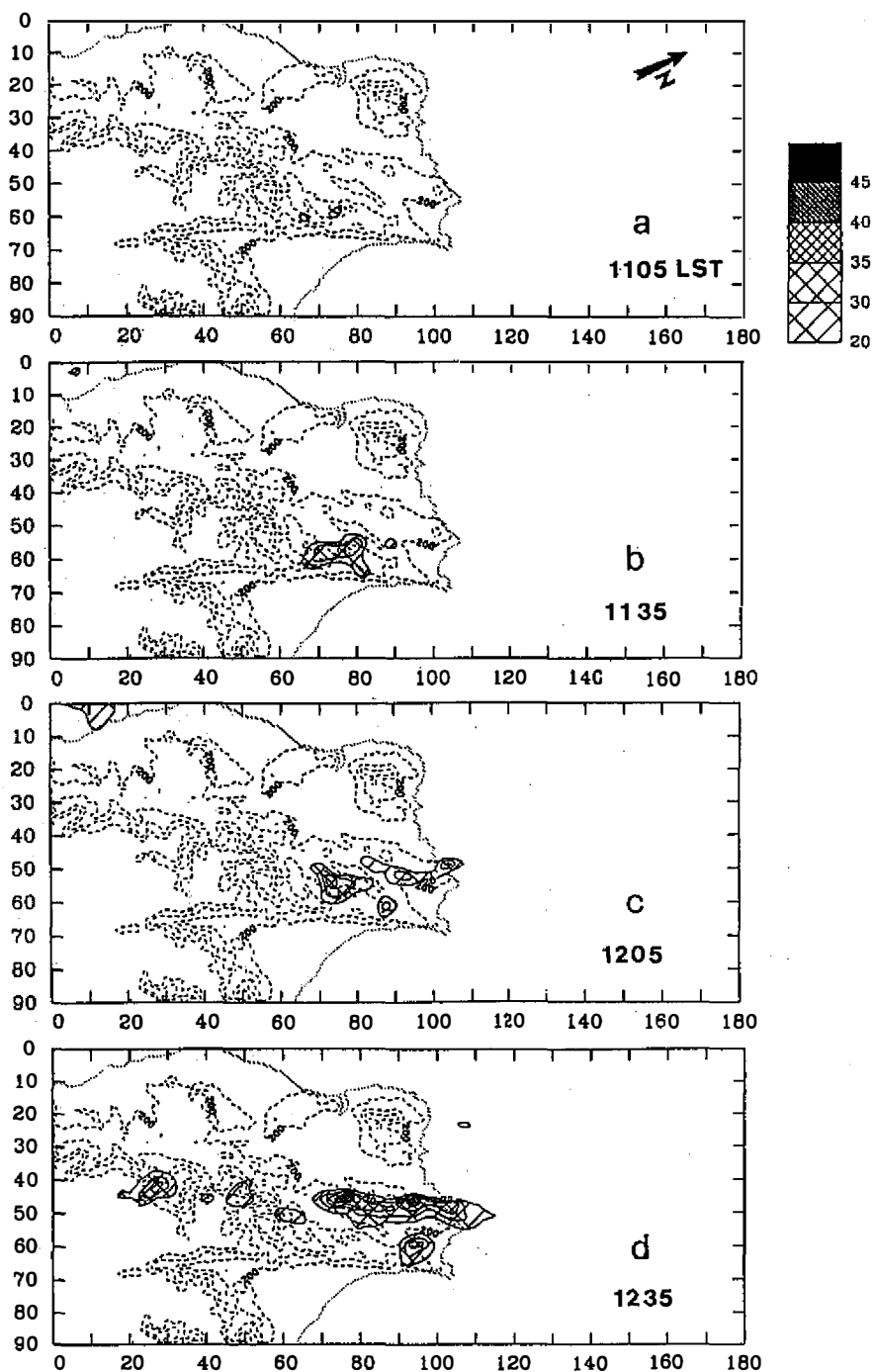
Fig. 4. Every 30 minute 3 km constant-altitude PPI (CAPPI) radar reflectivity
        maps from 1105 (a) to 1805 LST (o) 21 June 1991. The beginning
        contour is 10 dBZ. The contour interval is 10 dBZ. Heavily- shaded are
        areas with reflectivity larger than 45 dBZ. The broken lines are terrain
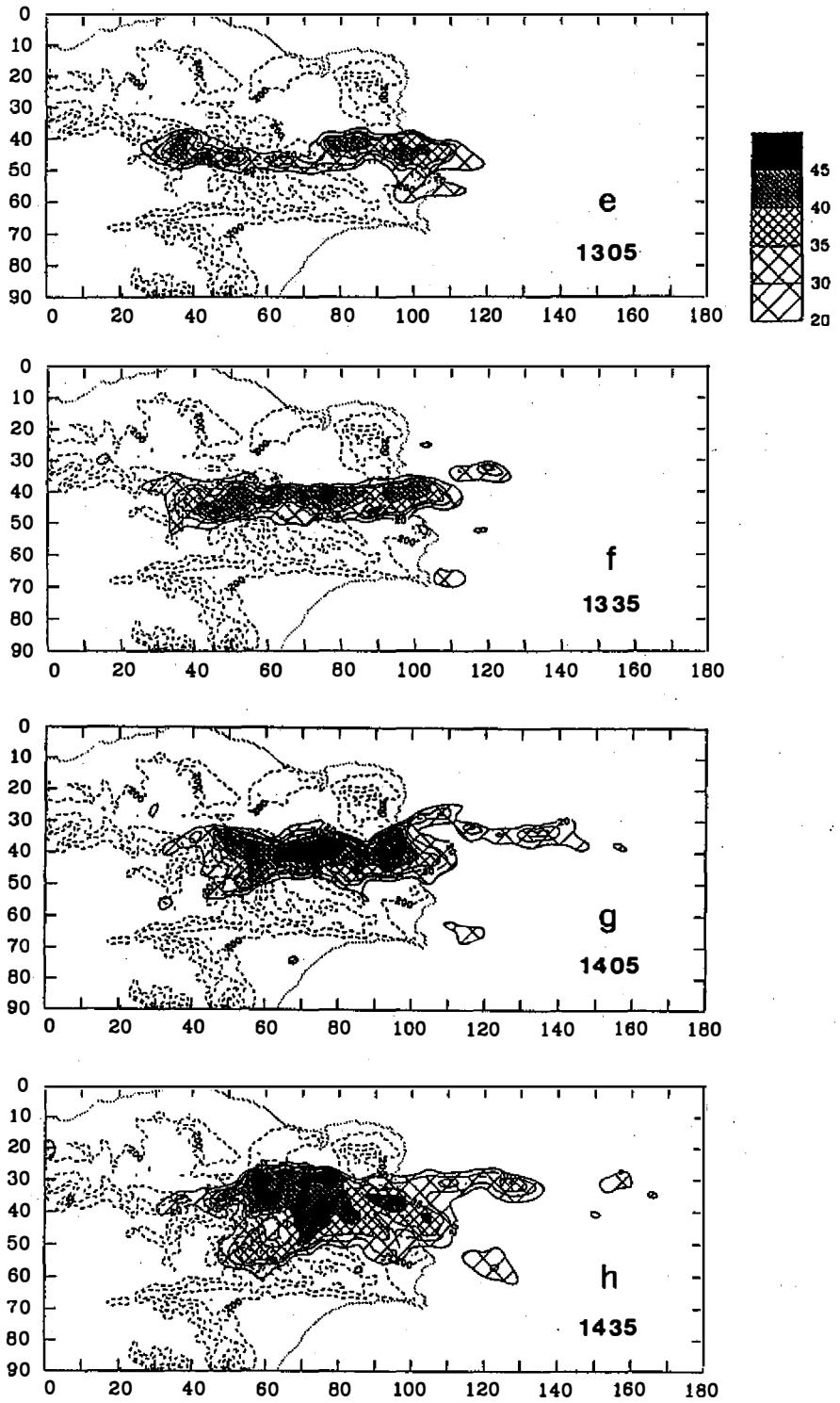   contours (200, 500, 1000, and 1500m, respectively).
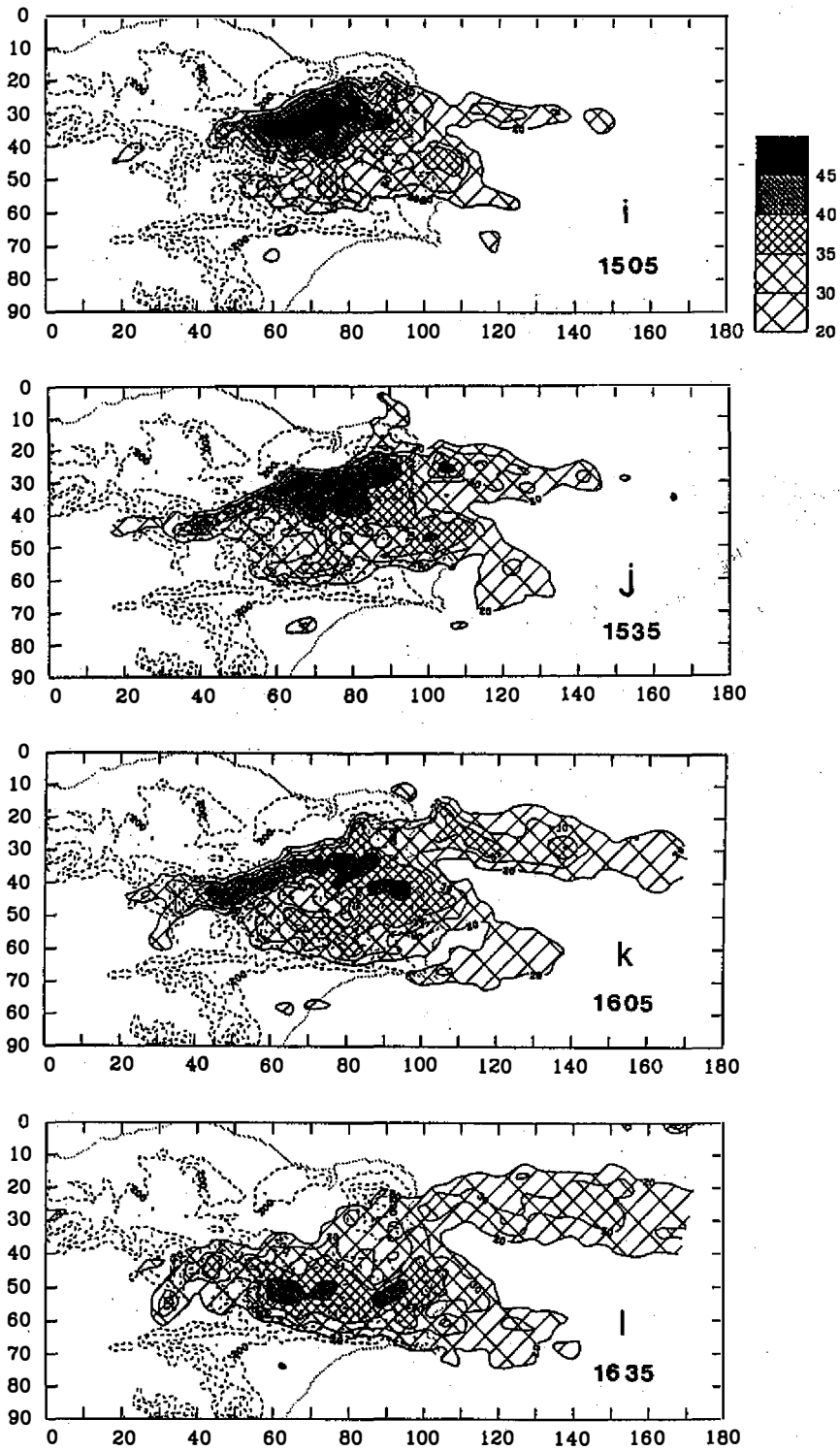
Fig. 4. (Continued.)
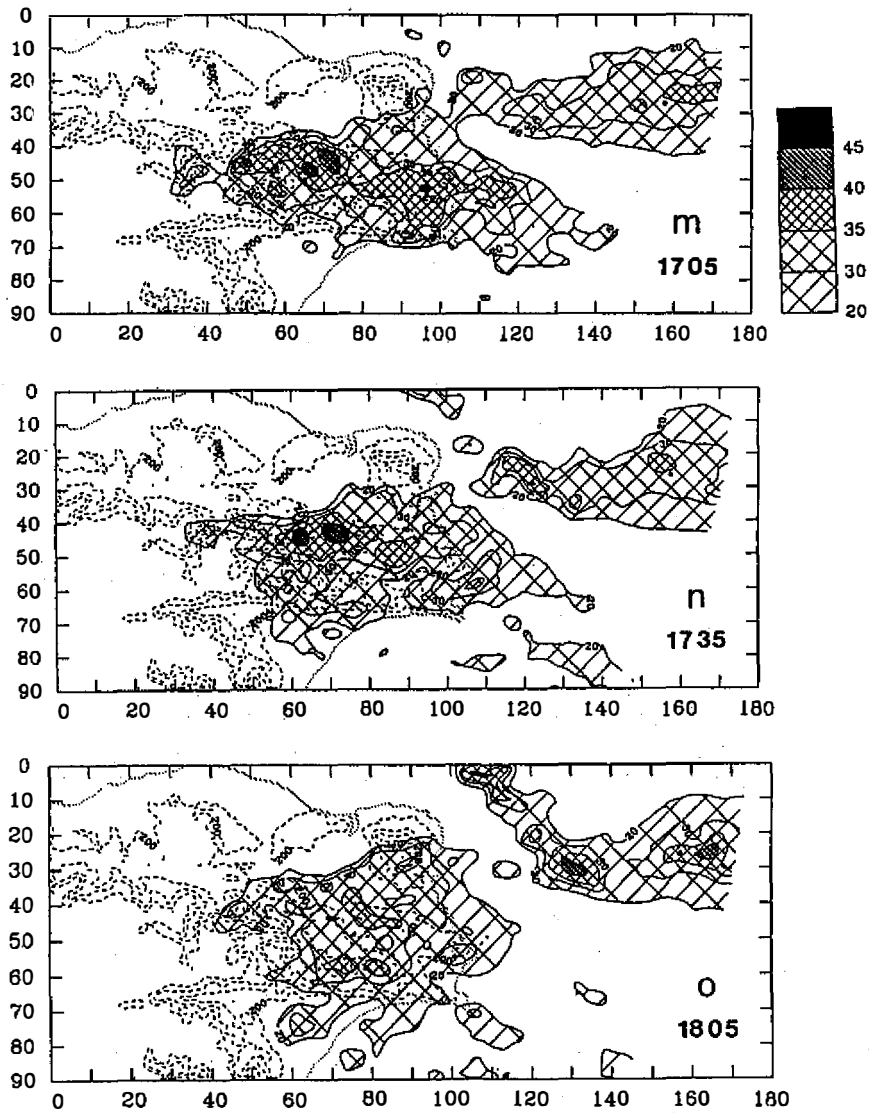
Fig. 4. (Continued.)

Fig. 4. (Continued.)

The propagation of each individual storm was investigated by time evolution of the maximum radar reflectivity in the vertical direction projected along a selected cross section. Figure 8a shows the cross section passing the Taipei basin and Keelong city in a northeast-southwest direction. The mean terrain feature is given at bottom of the figure. It can be seen storm C was initiated over the mountainous area south of Taipei and propagated, while developing, northeastward down the mountain slope. At 1405 LST, storm C arrived at the southern tip of the Taipei basin, and at the same time, the westward-propagating storm A also arrived in the Taipei basin from the east. Storm A and storm C merged together and produced large area heavy precipitation in the basin.

Figure 8b shows the time evolution maximum radar reflectivity cross section passing Taipei basin but in a northwest-southeast direction. It is clear storm A was initiated over
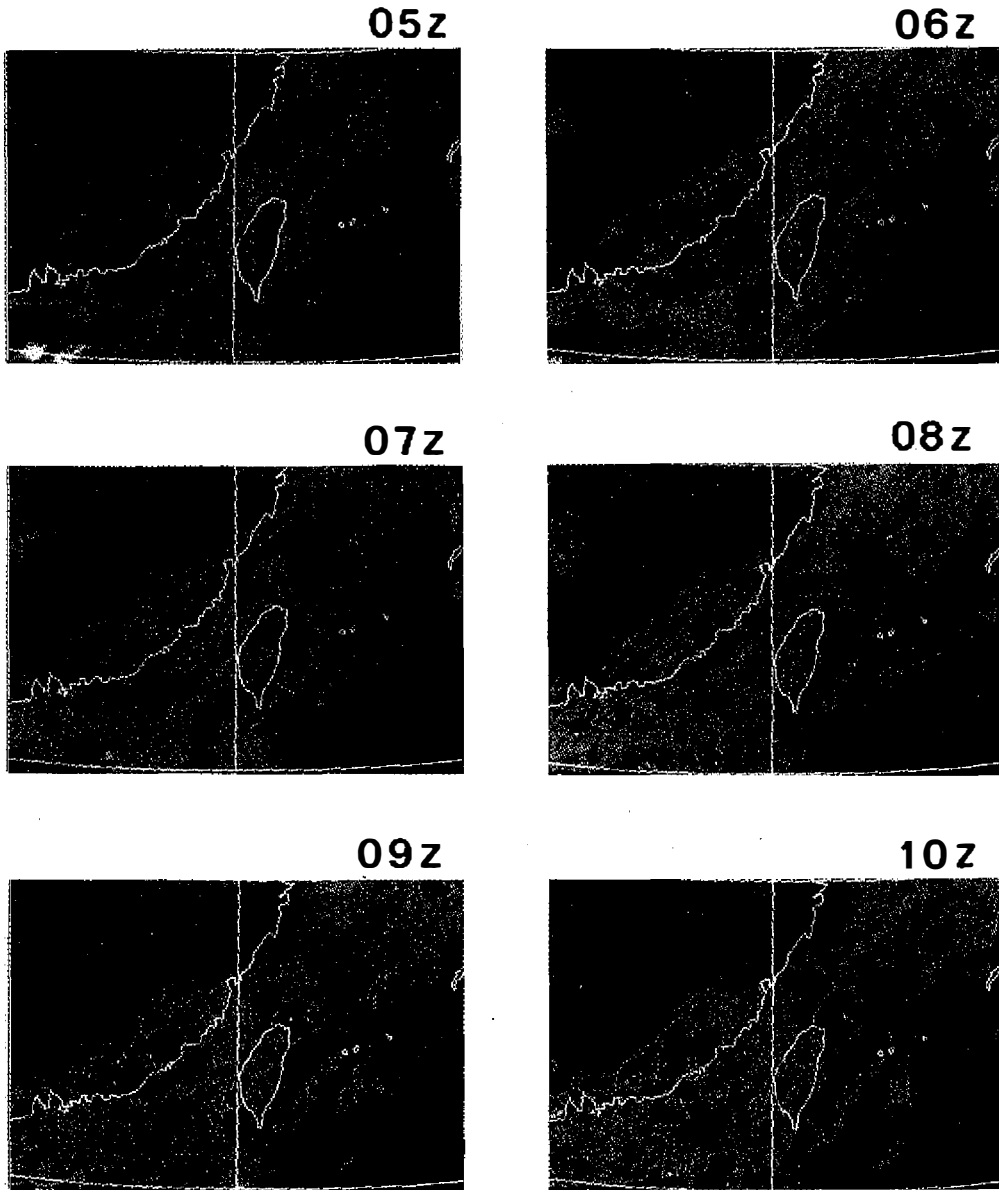
05z 06z

07z 08z

09z 10z

Fig. 5. Hourly enhanced GMS IR imageries from 05Z (1300 LST) to 10Z (1800 LST) 21 June 1991.
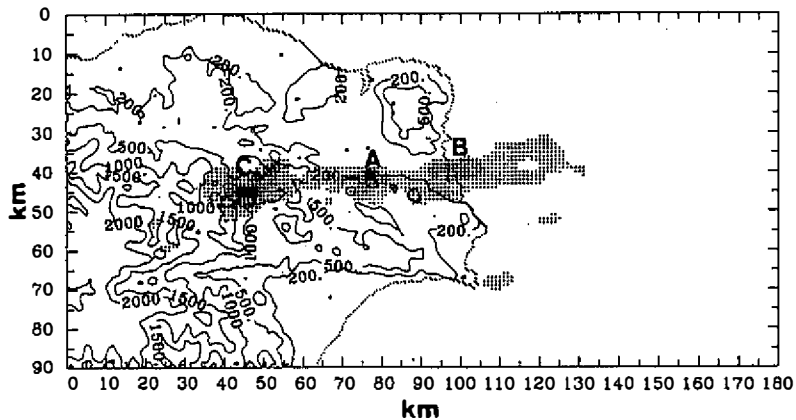
Fig. 6. Radar reflectivity map at 3 km height on 1335 LST 21 June 1991. The beginning shading is 30 dBZ. The dark shading represents radar echo larger then 45 dBZ. The thin lines indicate the terrain contours (200m, 500m, 1000m, and 1500m, respectively). The three major convective storms discussed in the text are indicated by A, B, and C.
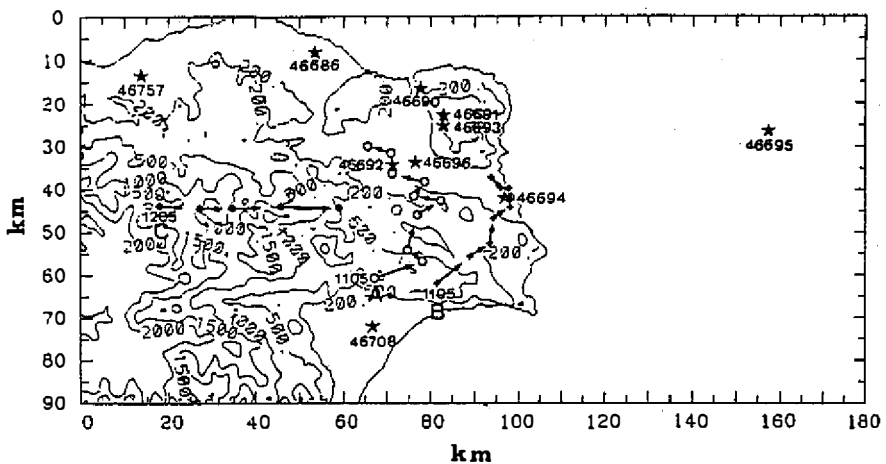

Fig. 7. Trajectories of the three major convective storms (A, B and C) on 21 June 1991 derived from the sequential radar reflectivity maps at intervals of 30 minutes.

the top of the mountains. At its early developing stage, storm A did not propagate much and only possessed weak echoes. Storm A started to move downslope when echo intensity exceeded 30 dBZ. The storm intensified significantly over the foothill area and reached its mature stage at about 1505 LST and maintained its strength till 1605 LST and then decayed afterwards. According to Taipei surface station observations (Figure 9), the storm brought 100 mm rainfall within an hour from 1453 to 1553 LST, and had its 10-minute maximum rainfall rate (23 mm/10 min) from 1515 to 1525 LST. The height-time indicator (HTI) of radar reflectivity across the Taipei station is also given in Figure 9. The reflectivity pattern indicates rain started to fall at 1400 LST. Deep and strong precipitation echoes moved into
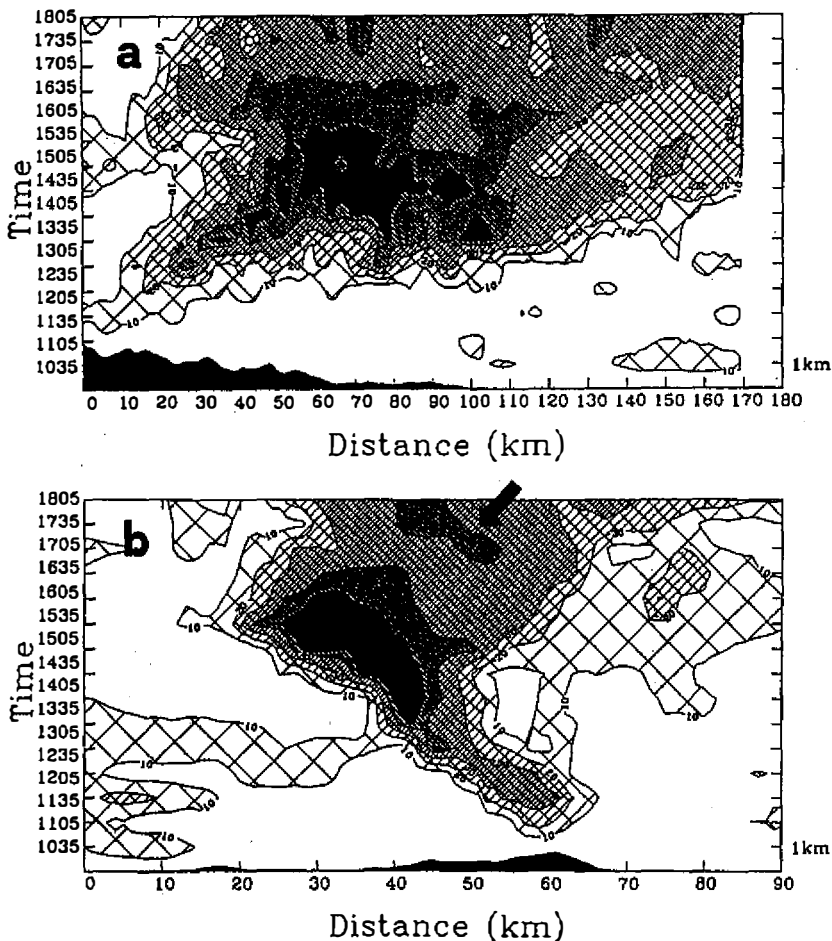
Fig. 8. Time evolution of maximum radar reflectivity in averaged cross sections passing the Taipei basin in (a) northeast-southwest (36-45 km) and (b) northwest-southeast (70-79 km) directions, respectively. The beginning contour is 10 dBZ and increase by 10 dBZ. The terrain feature is shown at the bottom of the figure.

the station at 1415 LST. Strong echoes lasted till 1600 LST. After a 30 minutes break period, weak stratiform precipitation echoes followed. There is a good comparison between the HTI reflectivity map and the surface rainfall measurement. While the storm system was passing by the Taipei surface station (1400-1515 LST), surface temperature at the station dropped from 30°C to 25.5°C ; the surface pressure increased from 999.8 hPa to 1001.8 hPa; and surface wind changed abruptly from westerly to easterly. All these observations indicate a strong cold pool of air associated with the heavy precipitation propagated across the station during this period. The cold pool air persisted with the heavy rain and had a character of high pressure, low temperature, and sudden change of winds. Similar phenonmena were observed by Charba (1974) in squall-line gust fronts; by Goff (1976) in thunderstorm outflows; and by Fankhauser (1976) in hailstorm systems. With high temporal and spatial resolutions of Doppler radar and rawinsonde data, Wakimoto (1982) studied the detailed life cycle of this type of thunderstorm
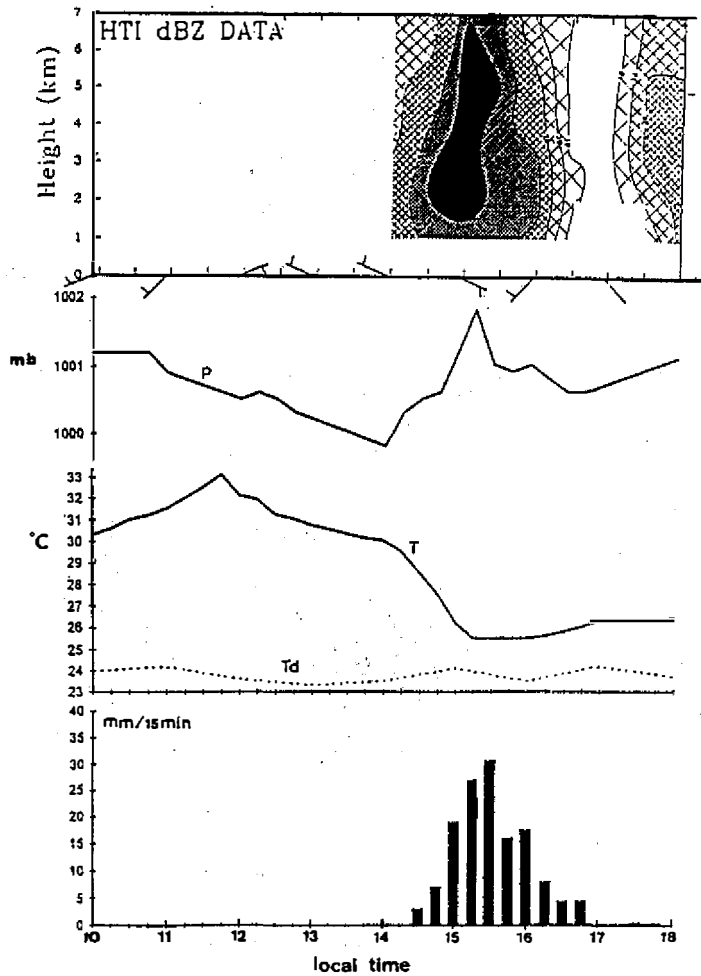
Fig. 9. Surface observations of winds, pressure, temperature, dew point, and rain-
fall intensity at Taipei station from 1000 to 1800 LST 21 June 1991. The
rainfall data is at 15-minute intervals and others are hourly data. On the
top of the figure, the corresponding height-time indicator (HTI) of CAA
radar reflectivity over Taipei station is also given.

outflows phenomena. It is known that the formation of this cold pool air with sudden wind
change is caused by convective downdrafts embedded within the convective precipitation
systems. The leading edge of this cold pool air forms the gust front that commonly produces
significant convergence and is favorable for triggering new convections. The possible role
of this mechanism in maintaining the storm system will be discussed later.

Figure 8b also showed there were newly-developed convections initiated in the moun-
tainous area at about 1530 LST (the arrow sign in Figure 8b). The convections propagated
westward to the basin at about the same speed as the main system but with a much weaker
intensity. From a preliminary study on the climatological characteristics of mesoscale pre-
cipitation systems in Mei-Yu season, it is suggested that the secondary development of con-
vections in late afternoon in mountainous areas in northern Taiwan is not an uncommon
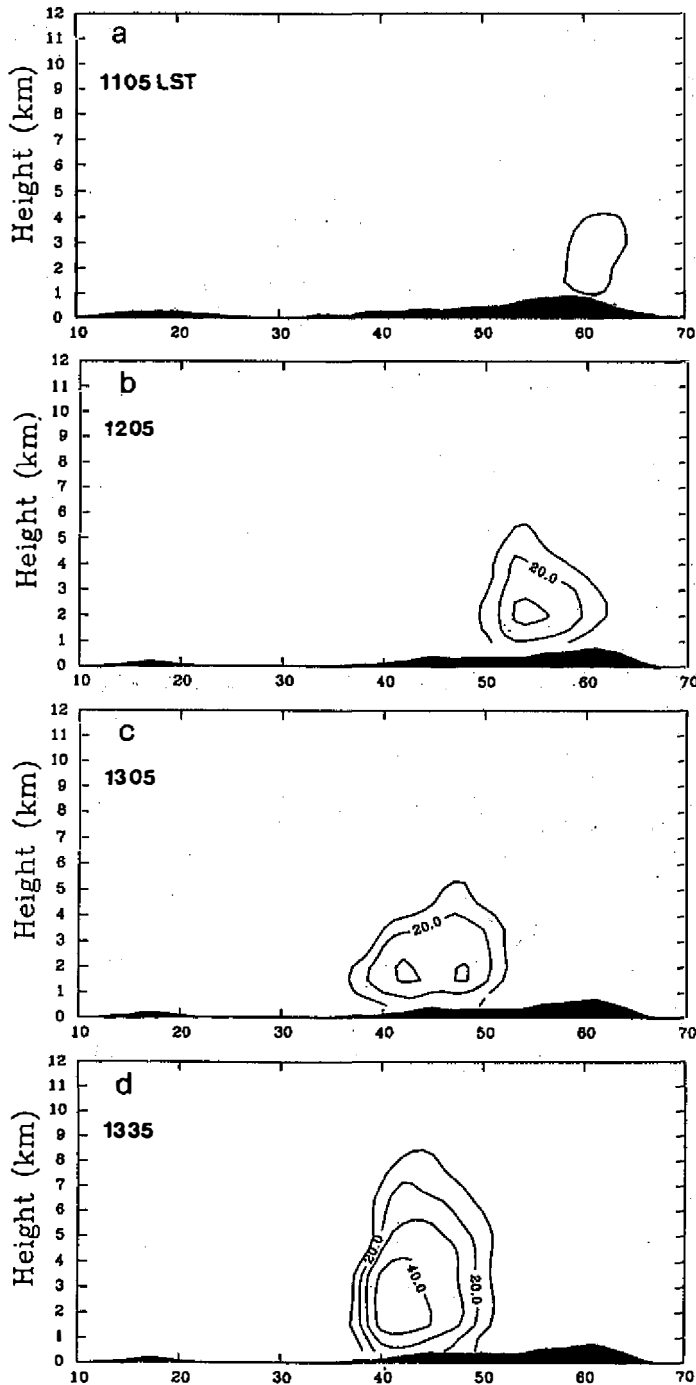phenomenon.

Fig. 10. A sequence of radar reflectivity maps derived from CAA Doppler radar at selected times on 21 June 1991. The cross sections are selected to pass the Taipei basin northwest-southeast. The beginning contour of reflectivity field is 10 dBZ and the contour interval is 10 dBZ. The mean terrain feature is shown at the bottom of the figure.
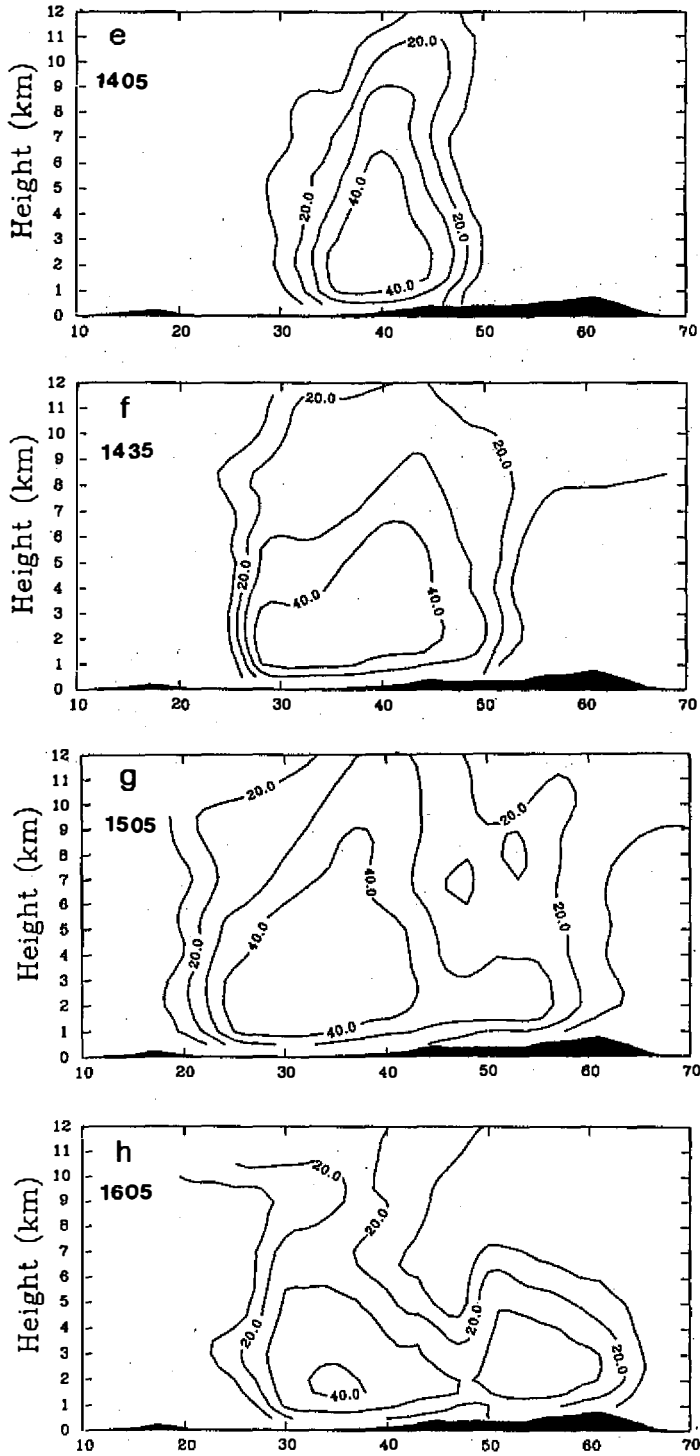
Fig. 10. (Continued.)

5. STRUCTURE AND EVOLUTION OF THE STORM

5.1 Precipitation Structure and Evolution

According to the major changes of the precipitation structure, the evolution of the mesoscale convective precipitation system can be divided into four stages, i.e., the early developing stage (1035-1305 LST), the rapidly intensifying stage (1335-1435 LST), the mature stage (1505-1605 LST), and the dissipating stage. A sequence of vertical cross sections of reflectivity field perpendicular to the storm are given in Figure 10. The cross sections are chosen to reveal the structure and evolution of the storm which brought the heavy rain to the Taipei basin. In the early developing stage, the convection was shallow with echo top (defined by 10 dBZ contour) below 6 km height. The first echo was observed over the mountain peak area at 1035 LST with very weak and shallow echo structure similar to what was shown in Figure 10a. After initiation, the storm developed gradually and propagated slowly westward down the mountain slope. During this period, the storm did not show significant development. The equivalent reflectivity factor reached 30 dBZ and had its maximum value at around 2 km height. The storm reached the foothill of the mountain at 1305 LST (Figure 10c). Two separated precipitation echo centers were observed at low level indicating a weak multicellular convective system.

The storm intensified rapidly when it arrived at the foothills. Within an hour (1305-1405 LST, Figures 10d and e), the major rain area of the storm extended vertically well above 12 km and the 30 dBZ reflectivity contour reached 9 km height. The reflectivity pattern shown in Figure 10e suggested the existence of deep convective updrafts in the storm. At this time, the maximum reflectivity of the storm was stronger than 45 dBZ and occupied a large area. In the rapidly intensifying stage, the storm showed an intense upright feature without significant overhang stratiform precipitation signature in the layer of outflows. The storm did not start to develop upper-level stratiform precipitation until 1435 LST (Figure 10f).

The storm reached its mature phase when the major convective precipitation region was largely in the Taipei basin (Figure 10g). The 30 dBZ reflectivity contour reached well above 12 km height and extended to 40 km wide horizontally. At this stage, as shown in Figure 4i, the high reflectivity region of the storm occupied the whole Taipei basin and the Keelong Valley and brought heavy rain to these areas. No well-organized stratiform rain area in the upper troposphere was observed and no signature of bright band was detected at this time. In the dissipating stage (Figure 10h), the convection in the basin area dissipated quickly, but the newly-developed convections were observed in the mountainous area at the same time. The newly-developed convections propagated downslope of the mountain with approximately the same speed as the first wave but with a much weaker intensity (see Figure 8b). This secondary development of convections in the mountainous area not only elongated the duration of the storm system but also brought significant rainfall to the foothill areas to the southeast of Taipei City in late afternoon (see Figure 1a).

5.2 Flow Structure and Evolution

In Figure 11, a sequence of vertical cross sections of horizontal winds perpendicular to the storm system derived from CAA Doppler radar's radial velocity data are given. Since the radial velocity only sampled a partial component of the true total velocity, the derived wind field could only be interpreted in a qualitative manner. The heavy-shading region is flow from right (called easterly wind for convenience) with magnitude less than 5 m s^{-1}, while

Date = 91/06/21   Time = 12:05:00

Date = 91/06/21   Time = 12:35:00

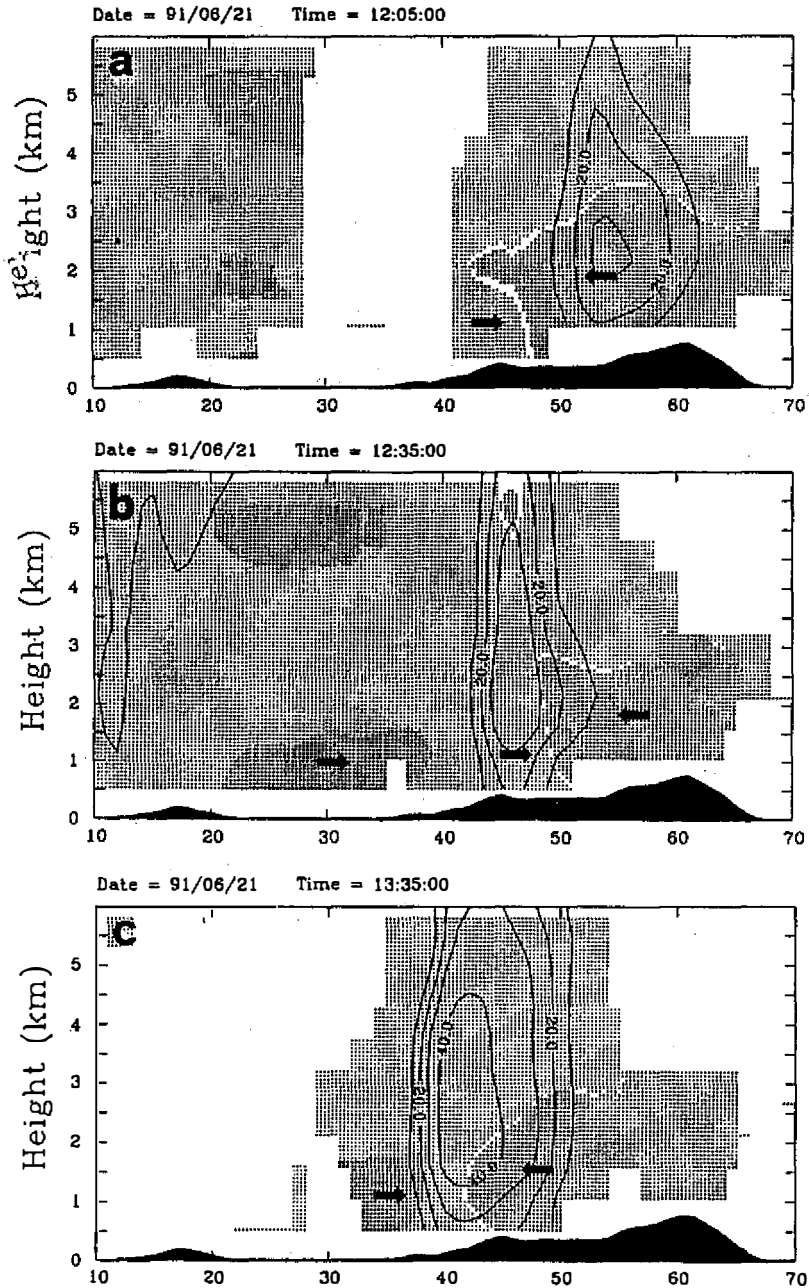Date = 91/06/21   Time = 13:35:00

Fig. 11. A sequence of horizontal winds perpendicular to the storm orientation, derived from the CAA Doppler radar's radial velocity data at selected time on 21 June 1991. The cross sections are selected to pass the Taipei basin in northwest-southeast direction. The heavy- shading represents flow from the east and the lighter-shading represents flow from the west with speed less than 5 m s^{-1}. Within the westerly flow regime, the heavier-shading represents flow from the west but with speed greater than 5 m s^{-1}. The mean terrain feature is shown at the bottom of the figure.
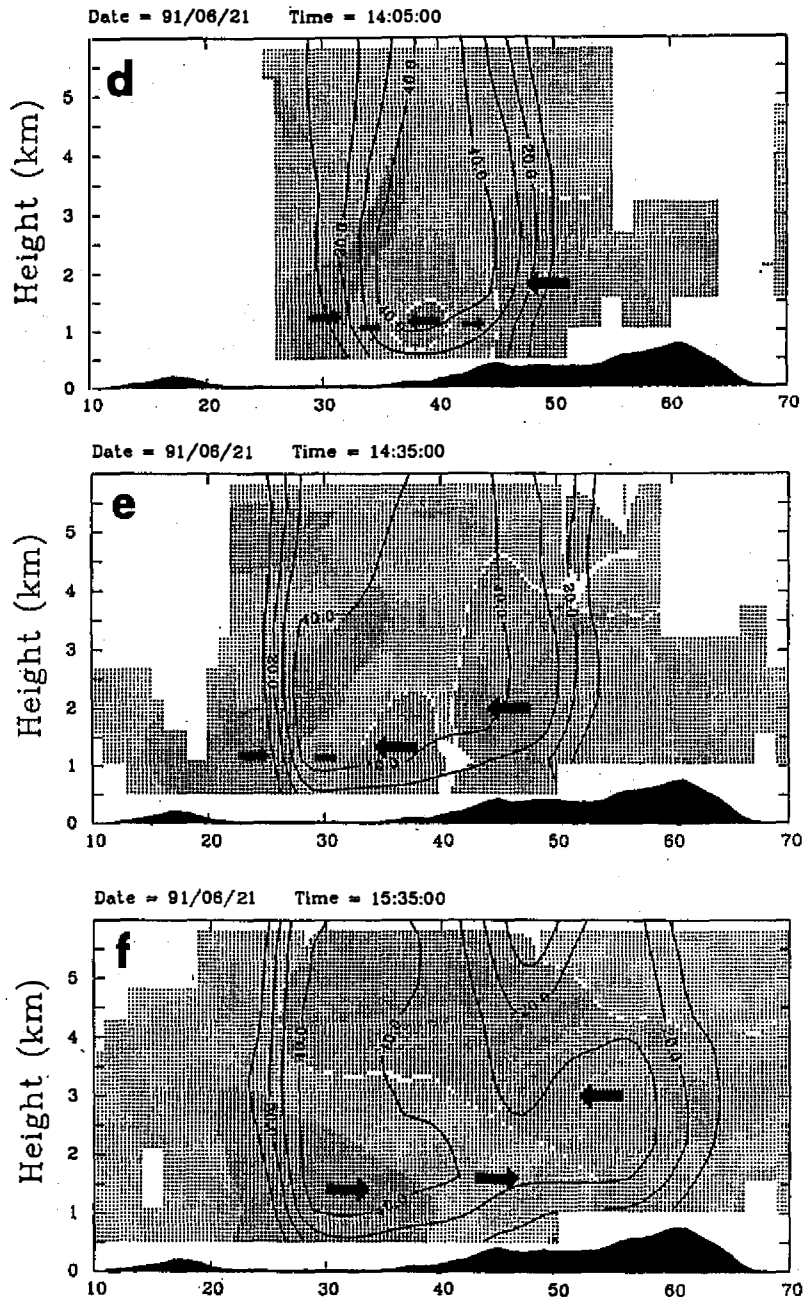
Fig. 11. (Continued.)

the lighter-shading region are flows from left (called westerly wind) with magnitude less than 5 m s^{-1}, respectively. Due to the inherent limitation of radar measurement and to avoid the unnecessary ambiguity possibly associated with the derived wind field, the discussion in the following will be focused on the low-level flows only. It is shown, in the early development stage (Figures 11a and b), the low-level flows revealed several different mesoscale features

during this relatively undisturbed period. Weak westerly winds prevailed in most of the troposphere over northern Taiwan in the late morning hours. Over the mountainous area, on the other hand, weak easterly winds were present in the lower troposphere. The shallow convection in the mountain was embedded in the low-level easterly flow regime and located at a position some distance away from the convergence line (In the plots, the convergence line was enhanced by the white color zone) . Over the western slope and the Taipei basin area, stronger westerly winds (> 5 m s^{-1}, heavier-shading) were detected by the CAA Doppler radar in the lowest 1.5 km after 1200 LST (Figure 11b). This stronger westerly wind occurred in the atmospheric boundary layer (ABL) and progressed inland in the middle of the day (see Figure 11c) **suggesting** the existence of the thermally-driven sea breeze. The leading edge of these stronger westerly winds reached the foothill of the mountain at around 1300 LST and was lifted along the sloping terrain (at x=40 km in Figure 11c).

The development of upslope winds along the western slope of the mountain was also detected by the Doppler radar as shown in Figure 11b. The leading edge of the westerly wind within ABL was at 47 km east of the radar at 1205 LST (Figure 11 a), and progressed upslope to the higher mountain range at 1305 LST. In summary, in the early development stage, the atmosphere was relatively undisturbed. At this time, the sea breeze over the foothills and the upslope winds at midslope were both present in ABL and were detected by CAA Doppler radar. The penetration of the upslope winds into the higher terrain provided a possible mechanism for mountainous convection development (Banta, 1990).

The flow structure revealed quite different mesoscale features in the rapid intensifying stage (Figures 11d and e). The sea breeze and upslope winds were both disturbed by the intensified convective motions. The leading edge of the sea breeze (suggested by the stronger westerly winds in the ABL) was lifted to a higher altitude by the storm indicating the existence of the intense convective updrafts at the front portions of the storm system. Notice that the storm was moving west. Accompanying the uplift of the sea breeze, the winds in ABL over the foothill abruptly changed from strong westerly to weak easterly (at near x=40 km). This abrupt change of winds coincided with strong convective precipitation echoes associated with the storm. The observations indicated by the surface station, as shown in Figure 9, suggest the existence of pronounced convective downdrafts within the storm. In summary, the intensifying storm system had its major convective updrafts on the leading edge of the storm and its major convective downdrafts just behind the updrafts. The updrafts tilted rearward (to the east) with height as inferred from the eastward tilt of the stronger westerly flows. The downdrafts produced pronounced outflows underneath the heavy precipitation area. Enhanced local convergence in ABL at the front portions of the storm induced by the storm-generated outflows and the local sea-breeze and the upslope winds (as shown in Figures 11d and e) seemed to be important to the maintainence of the storm system.

In the mature and dissipating stages, the low-level flows were dominated by the precipitation loading-induced outflows (Figure 11f). No pronounced uplift of the low-level westerly wind was observed indicating the diminished convective updrafts. These features are consistent with what has been observed in a dissipating thunderstorm.

6. DISCUSSION

In the late morning of 21 June 1991, a convective precipitation system developed in the mountainous area of northern Taiwan. The convective precipitation system organized into a NE-SW oriented mesoscale line feature along the western mountain slope at a later

time. More than 120 mm rainfall poured down on the cities of Taipei and Keelong within 3 hours. The storm initiated, developed, organized, and dissipated within the detection limit of a C-band Doppler weather radar on the northwest coast of Taiwan. In this paper, the role of mountains on organization and propagation of the mesoscale precipitation system was studied by using the Doppler radar data.

The storm initiated at the mountain peak area, propagated down the terrain slope, and brought heavy rain to the basin and plain areas. In the early stage, the precipitation system developed along the mean low-to-middle tropospheric winds into a NE-SW convective line. When precipitation-induced outflows occurred, the interaction between the upslope winds and the storm-generated outflows dominated the storm propagation. Reaching the foothills of the mountain, the storm intensified dramatically. In the basin area, the interaction between storm-generated outflows and the environmental low-level flows dominated storm development. At this stage, the storm was quasi-stationary. Deep cumulonimbi continually reformed over the southwest quadrant and move northeastward and produced copious rainfall in the same region.

It is interesting to note that the convections developed along the mean wind direction initially. The low-level convergence line derived from the Doppler radial winds indicated that the convection was not colocated with the convergence line initially. It is unlikely the development was mainly due to mechanical lifting since the mean wind was almost in the same direction of the CMR. By examining the vertical profile of radar reflectivity associated with the storm, the convection was not strong and mainly along the mountain peak in the early development stage. Surface observations from Taipei station indicated that there was plenty of surface solar heating in the morning and surface temperature increased about 7°C within 3 hours. These observations seemed to suggest that the convection on the mountain peak were possibly triggered by thermal forcing at the early stage. Cumulus clouds triggered by mixed layer thermals in the convective boundary layer is an important mechanism of cumulus cloud initiation in warm season (Stull, 1988). Local convecgence induced by elevated heating at the mountain top is another possible mechanism. Further investigations are needed in order to clarify the role of thermal forcing and orographic lifting in cumulus convection initiation near the mountain top in northern Taiwan.

Chen *et al.*(1991) studied the effect of mountains on mesoscale precipitation system in northern Taiwan using TAMEX data set (IOP 8). In the case studied, the new convective cells formed over the sloping area west of the mountain crest and propagated eastward to the mountain peak. The new cells merged with the old cells over the mountain range. The heavy rain was brought to the sloping terrain and mountainous areas. In the present case, the convective cells initiated in the mountainous areas and propagated westward down the sloping terrain. The convection was intensified when it approached the foothills. The heavy rain was brought to the foothills and the basin. The behavior of these two storms is quite different. In Figure 12a the reconstructed winds from soundings of Panchiao taken from 0800 LST, 7 June 1987 (TAMEX IOP 8) is given. The u-component is perpendicular and the v-component is parallel to the storm orientation, e.g., 45° clockwise from the north, In the 7 June case, the vertical wind shear was westerly and with moderate intensity. The eastward propagation of the storm toward the mountain indicated the downshear development and is consistent with the early modeling works. In the 21 June 1991 case (Figure 12b), the shear vector at low level was easterly and very weak. The convective cells initiated on the mountain peak, possibly due to elevated solar surface heating, primarily propagated in the direction parallel to the environmental flows, i.e. northeast. While the storm became precipitating, the storm-generated outflows had its strongest component in the direction down the mountain
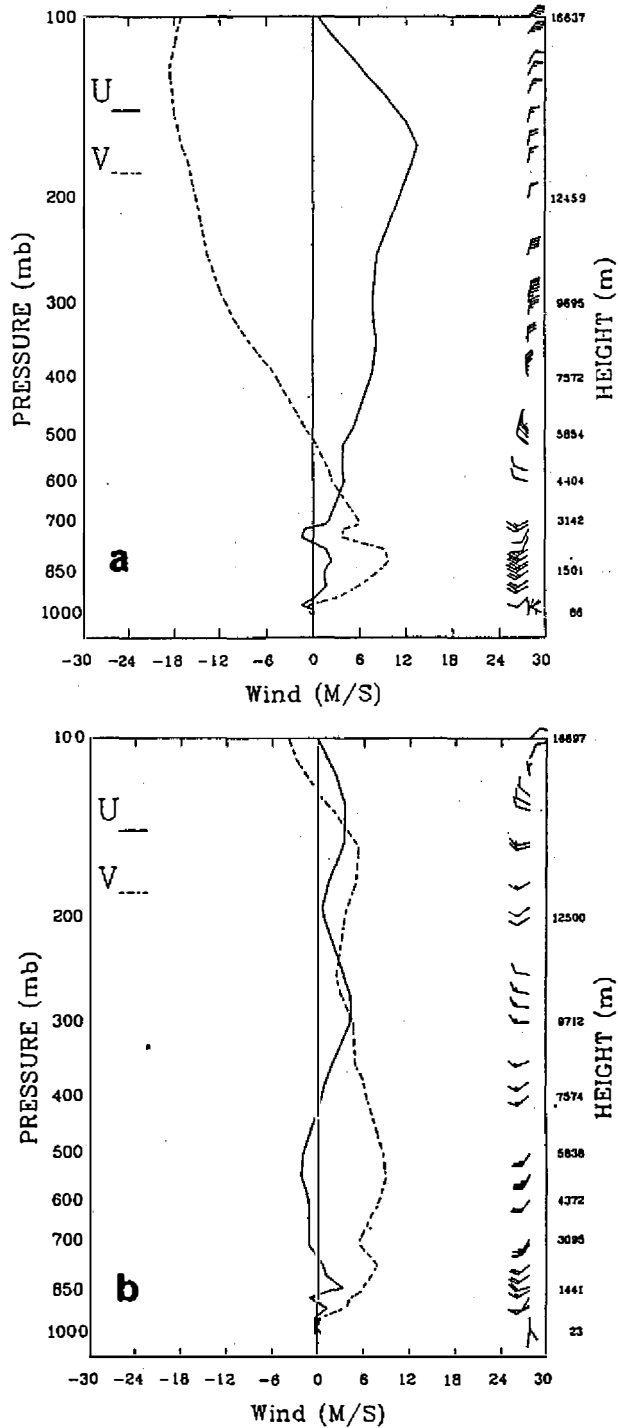
Fig. 12. The components of wind perpendicular (u) and parallel (v) to the storm
orientation taken from the sounding at Panchiao on (a) 0800 LST (00Z)
7 June 1987, and (b) 0800 LST (00Z) 21 June 1991, respectively.

slope. New convective cells were apt to develop in the leading edge of the outflows which were evidenced by the maximum gradient of radar echoes. Thus, the storm propagated in the north-northwest direction if the cells were initiated east of the Taipei basin, and in the northeast direction if the cells were initiated south of the Taipei basin.

The storm intensified dramatically while moving toward the foothills. This suggests, in section 5, that the inland penetration of the sea-breeze might play an important role in intensifying the storm by strengthening the convergence upslope. In the basin area, the storm attained its mature stage, heavy rain produced a large area of cold pool air associated with pressure rise and wind shift was observed. At this period, the storm revealed a quasi-stationary character and propagated very slowly toward west-southwest. At this time, there was no sloping terrain effect. The most favorable location for new convective cells to form was the region where the fresh, warm and moist air existed, i.e. the southwest quadrant of the storm. The developing cells moved northeastward along the prevailing winds and merged with the major convective system and greatly increased the precipitation.

The vertical structure of the convective precipitation system was also examined in this study. The strong reflectivity region in the storm was first found at about 2 km height in the early developing stage and extended upward well above 12 km height. The convective updrafts, inferring from the uplift of the westerly momentum in the middle troposphere associated with the penetrated sea breeze circulation, tilted slightly downshear at the leading edge of the storm. The existence of convective downdrafts located just behind the updraft region was also indicated by the Doppler radar observations of pronounced precipitation-induced divergence outflows near the surface. This inference was also confirmed by the observations at the surface station in the Taipei basin.

The stratiform precipitation region at the rear portions of the major convective precipitation region was observed but in a much weaker intensity and less organized fashion. The formation mechanism and the flow structure associated with the trailing stratiform precipitation area in a midlatitude squall-line system was discussed in detail by Smull and Houze (1987). They showed that, within the stratiform area, there is a layer of upward-sloping, front-to-rear flow emanating from the upper portions of the convective line. This flow, which contains mesoscale ascending motion, advects ice particles detrained from the convective cells rearward. The ice particles slowly fall as they are carried rearward eventually to form aggregates. The aggregates fall through 0°C level and melt, producing the radar bright band. The slightly strengthened westerly flows in the stratiform precipitation region shown in Figure 11 suggested the presence of mesoscale upward-sloping flow in the rear portions of the storm. The reflectivity field, however, did not show any evidence of bright band in this case. The role of ice phase precipitation processes in the storm evolution in this case can not be clarified in the present context.

7. CONCLUSIONS

In this study, a mountain-originated mesoscale precipitation system in northern Taiwan was investigated. The movement and propagation of the storm system was delineated by using single Doppler radar located at CKS International airport. The structure and evolution of convections associated with the precipitation system was also examined. The interactions among the environmental winds, the sea-breeze circulation, the mountain-induced sloping winds, and the precipitation-induced outflows are discussed.

To summarize, the cumulus convection was triggered by thermal forcing on the mountain top. In the early developing stage, the storm propagation was mainly controlled by the translation process, i.e., propagated along the prevailing southwestly flows and gradually formed into a NE-SW line. The trajectory of each major convective storm was modulated by the sloping terrain. The modulation became effective while significant precipitation occurred. The precipitation-induced outflow had its largest component in the direction of terrain slope. The outflows interacted with the mountain-induced upslope winds to provide the necessary lifting for new convections to form on the west side of the old storm. Storm propagation at this stage was a result of combined effect of forced mechanism (mountain-induced upslope winds) and the autopropagation mechanism (storm-generated outflows). The storm moved to the foothill area at its mature stage. Enhanced convergence produced by the inland-penetrated sea breeze and the storm-generated outflows and abundance of low-level moisture associated with the sea-breeze circulation intensified the storm dramatically and produced significant rainfall over the basin area. The storm was almost stationary in the basin area. Sloping terrain has no role at this stage. The interaction between the storm-generated outflows and the low-level environmental flows (the sea breeze) favored new convective cells to form in the southwest quadrant of the system. A combination of the translation process (developed convective cells propagated along the mean wind toward northeast) and the autopropagation process (new convective cells formed at southwest of the storm) resulted in a near-stationary storm propagation. New convective cells merged with the old cells along the same trajectory, hence, brought the heavy rain to the same area in a short time.

From the above discussion, we have seen that the complex terrain features in northern Taiwan play a subtle role in controlling the organization, propagation, and development of the mesoscale convective precipitation systems over the area. We have provided some observational evidences of terrain effect on the precipitation systems using data diagnosis methodology. The capability of Doppler radar in revealing the important mesoscale features associated with the multicellular convective precipitation system is clearly demostrated here. It is not clear, however, which processes are most important under different environmental conditions. A comprehensive observational and numerical simulation study is urgently needed in order to get a better understanding of all these complicated mesoscale processes in the complex terrain of northern Taiwan.

<div align="center">REFERENCES</div>

Banta, R. M., 1990: The role of mountain flows in making clouds. Atmospheric Processes over Complex Terrain, Meteorological Monograph, Am. Meteor. Soc., William Blumen (Ed.), Chapter 9, 229-284.

Charba, J., 1974: Application of gravity current model to analysis of squall line gust front. *Mon. Wea. Rev.,* **102**, 140-156.

Chen, C.-S., W.-S. Chen, and Z.-S. Deng, 1991: A study of a mountain-generated precipitation system in northern Taiwan during TAMEX IOP8. *Mon. Wea. Rev.*, **119**, 2574-2606.

Cotton, W. R., and R. A. Anthes, 1989: Storm and Cloud Dynamics. Academic Press, San Diego, 883pp.

Durran, D. R., and J. B. Klemp, 1982: The effect of moisture on trapped mountain lee waves. *J. Atmos. Sci.*, **39**, 2490-2506.

Fankhauser, J. C., 1976: Structure of an evolving hailstorm, Part II: Thermodynamic structure and airflow in the near environment. *Mon. Wea. Rev.*, **104**, 576-587.

Gamache, J. F., and R. A. Houze, Jr., 1982: Mesoscale air motions associated with a tropical squall line. *Mon. Wea. Rev.*, **110**, 118-135.

Goff, R. C., 1976: Vertical structure of thunderstorm outflow. *Mon. Wea. Rev.*, **104**, 1429-1440.

Johnson, R. H., and J. F. Bresch, 1991: Diagnosed characteristics of precipitation systems over Taiwan during the May-June 1987 TAMEX. *Mon. Wea. Rev.*, **119**, 2540-2557.

Kuo, Y.-H., and G. T.-J. Chen, 1990: The Taiwan Area Mesoscale Experiment (TAMEX): An overview. *Bull. Am. Meteor. Soc.*, **71**, 488- 503.

Smull, B. F., and R. A. Houze, 1987: Dual-Doppler radar analysis of a midlatitude squall line with trailing region of stratiform rain. *J. Atmos. Sci.*, **44**, 2128-2148.

Stull, R. B., 1988: An Introduction to Boundary Layer Meteorology. Kluwer Academic Publishers, Dordrecht, 666pp.

Sun, W. Y., J. D. Chern, C. C. Wu, and W. R. Hsu, 1991: Numerical simulation of mesoscale circulation in Taiwan and surrounding area. *Mon. Wea. Rev.*, **119**, 2558-2537.

Wakimoto, R. M., 1982: The life cycle of thunderstorm gust fronts as viewed with Doppler radar and rawinsonde data. *Mon. Wea. Rev.*, **110**, 1050-1082.